Structural Studies of a Protocadherin-15 Fragment Essential for Hearing

A thesis presented

By

Conghui Chen

To

The Committee on Degrees in Chemistry ad Biochemistry

In partial fulfillment of the requirements
For a degree of
Bachelor of Science with Research Distinction
In the field of
Biochemistry

Research Advisor: Dr. Marcos Sotomayor, Assistant Professor of Department of Chemistry and Biochemistry
Defense Committee: Dr. John Shimko, Chemistry Lecturer of Department of Chemistry and Biochemistry

The Ohio State University
Columbus, Ohio

April 13th, 2016

Statement of Research

I conducted the research presented in this thesis under the professional guidance of Dr. Marcos Sotomayor of The Ohio State University Main Campus Chemistry and Biochemistry Department. I joined the Sotomayor lab in August of 2013, during my second year at the university. I was trained in the process of protein purification and cell culture by visiting graduate student Deryanur Kilic in conjunction with Dr. Sotomayor. Dr. Sotomayor offered knowledgeable tutelage in designing and performing the experiments, analyzing data, and the writing of this thesis. All molecular modeling and analysis was performed with the guidance and assistance from Dr. Marcos Sotomayor and Dr. Raul Araya-Secchi. My research was generously funded by The Ohio State University Chemistry and Biochemistry Undergraduate Research Scholarship from autumn 2013 until spring 2015. I performed research as part of the Biochemistry 4998 and 4999 courses as a requirement for the completion of the thesis.

Abstract

Sound travels through the external and middle ear to the fluid-filled cochlea where mechanosensitive hair cells transform it into electrochemical signals. On the apical side of each hair cell, a set of hair-like protrusions, called stereocilia form a bundle with filamentous connections (tip links) that are essential for hearing. In response to the mechanical force generated by sounds waves, stereocilia move back and forth, thereby stretching tip links and opening nearby transduction channels. The tip link is formed by two non-classical cadherins, Cadherin-23 (CDH23) and protocadherin-15 (PCDH15), which are members of the cadherin superfamily of calcium-dependent adhesion proteins. CDH23 has 27 extracellular cadherin (EC) repeats and PCDH15 contains 11 EC repeats. Single missense mutations in PCDH15 are known to cause deafness, and absence of this protein leads to both deafness and blindness. A recent study showed that a point mutation (V767-) located in the PCDH15 EC7 repeat is pathogenic. My project focuses on determining the structure of the PCDH15 EC7 to EC8 fragment via X-ray crystallography, both to understand its function in hearing and to discover the structural effects of pathogenic mutations.

In a first step to achieve these goals we used a DNA construct that encodes for the mouse PCDH15 EC7-8 fragment to express it in a bacterial system. After transformation and culture, we successfully observed protein expression. However, the protein fragment was not soluble and aggregated in inclusion bodies. Therefore, I did protein purification under denaturing conditions, followed by refolding and size-exclusion chromatography, and obtained pure folded protein amenable for crystallization. I obtained protein crystals that diffracted when exposed to X-rays

and then refined the crystallization conditions to obtain a full data set with a resolution of 2.0 Å. Using this data set I found a molecular replacement solution for the first crystal structure of PCDH15 EC7-8, which I am currently refining. In this thesis I will describe each of the steps involved in obtaining the structure of PCDH15 EC7-8 and will discuss how the study of this structure will help us understand the mechanisms of mechanotransduction in normal and impaired hearing.

Acknowledgments

First and foremost, I would like to extend the sincerest of thanks to my thesis advisor Dr. Marcos Sotomayor for all of the efforts that he has put into making my time in his lab one of the most rewarding and exciting experiences of my life. Dr. Sotomayor's dedication and commitment to education and science influence me every time we interact. No matter how busy or crazy his schedule is, he will always answer all of my questions and offer steadily help with all support. More importantly, he always encourages me to take challenges and raise questions to perfect me to a better person. It is truly my pleasure and privilege to be one of his students, and I hope that one day I will be able to live up to the example that he has set for me over the past three years.

I would also like to extend thanks to Carissa Klanseck for collaborating with me on this project. She is a thoughtful and generous former undergraduate student and gave me support that allowed me to be able to achieve the results presented in this thesis.

I would also like to give huge thanks to Dr. Raul Araya-Secchi, the post-doctoral fellow that I worked with alongside for 2 years. I would like to thank him for his generous support of sharing his structure with me so that I can achieve my final structure. He is a person full of knowledge and helpful for assisting me with any technical issues whenever I confront any.

I would like to thank all of my generous and kind research co-workers in the Sotomayor lab. It is your endless support and help that makes me to be me today.

Besides working in the lab, we also are becoming lifelong friends with each other, which is a very precious experience and time to me.

Last but not at least, I would like to give thanks to The Ohio State University for offering me scholarships for the past two year that gave me inspiration and support during school years.

Table of Contents

Figures Index

Tables Index

Chapter 1: Introduction

Hearing, as the ability to perceive sound by detecting vibrations, is considered to be one of the most important sensations in all-living organisms and in humans. However, deafness is found to be the most common loss of perception as it affects more than 40 million people in the United States[1]. Deafness, an aetiological heterogeneous trait, is caused by various genetic and environmental factors[2]. It does not only have a great influence in one's life, but also impacts the whole family[3]. Hearing loss has been observed in up to 20% of 10 year-old children[4]. Unfortunately, it is often hard to diagnose and treat auditory disease because the sensory hair cells do not have the ability to regenerate[3,5].

Potential hearing loss treatments have been discovered, such as partial deafness treatment (PDT), which utilizes both electrical and acoustic stimulation to enable hearing[6]. Nonetheless, our knowledge of hearing impairment is very limited and genetic treatments for hearing loss have not been successfully developed yet. To elucidate the mechanism of some forms of hereditary deafness, we want to take an in-depth look at the structure of a non-classical cadherin, protocadherin-15 (PCDH15), which is crucial for auditory mechanotransduction[7,8]. Therefore, I will first introduce the role of PCDH15 in normal hearing and the basics of the cadherin family in Chapter 1. Next, I will discuss how I produced and purified a fragment of PCDH15 (EC7-8) in Chapter 2. In Chapter 3, I will illustrate the process of protein crystallization and data collection. Finally, I will analyze the preliminary structure of protocadherin-15 EC7-8, its calcium-binding motifs, its mutation sites related to deafness, and its possible interfaces.

1.1 Hearing, mechanotransduction, and the tip link

Sound travels from the outer ear through the external auditory canal to the tympanic membrane causing it to vibrate. The eardrum then propagates the vibration to the ossicles, where the sound energy is transmitted over to the oval window at the entrance of the cochlea (Fig. 1). The cochlea, a spiral-shaped, fluid-

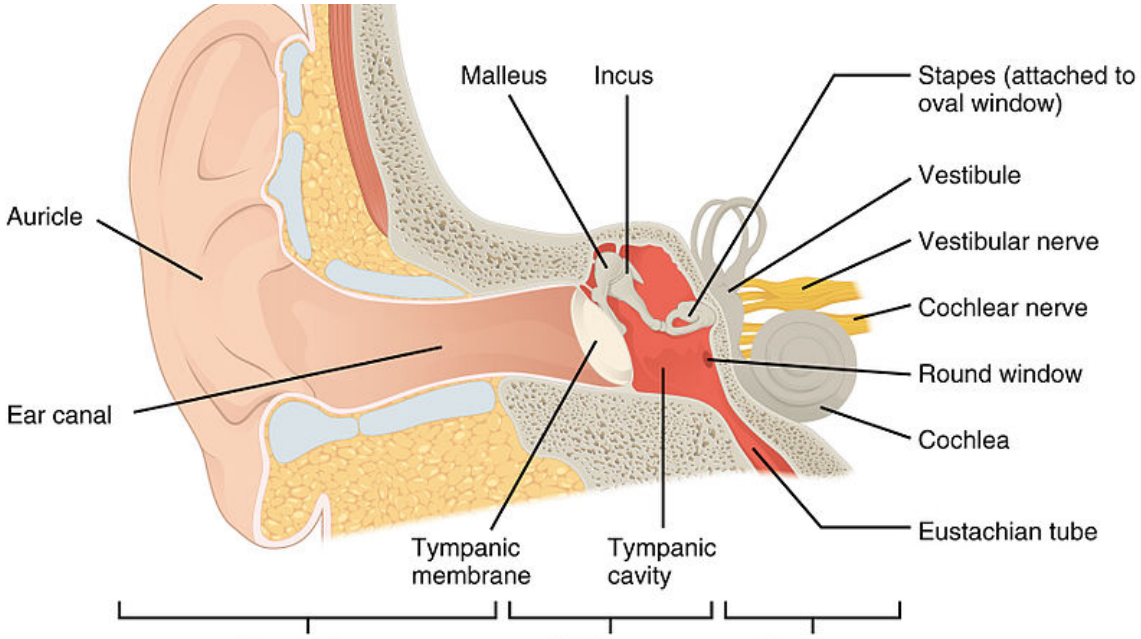

Figure 1: The external ear contains the auricle, ear canal, and tympanic membrane. The middle ear contains the ossicles and is connected to the pharynx by the Eustachian tube. The inner ear contains the cochlea and vestibule, which are responsible for audition and equilibrium, respectively. From [32].

filled organ embedded in the temporal bone, houses the basilar and tectorial membranes and the organ of corti where mechanotransduction takes place. The sound energy causes oscillation of specific regions of the basilar and tectorial membranes (Fig. 2).

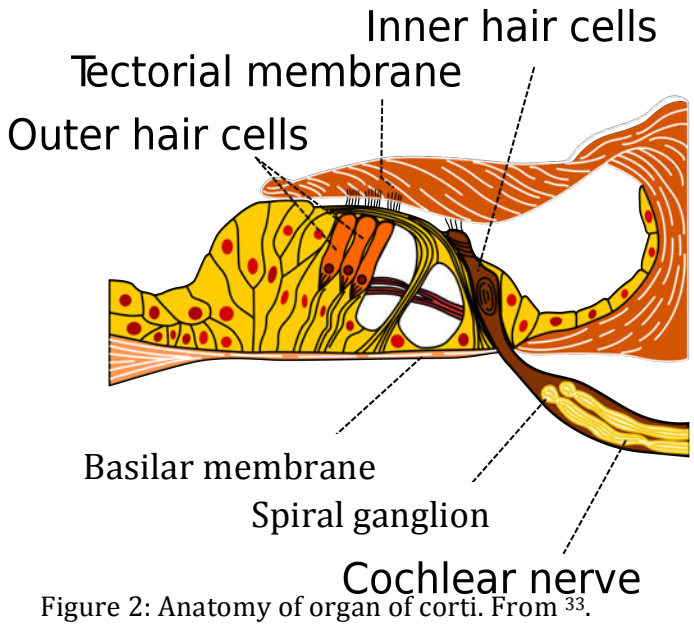

Figure 2: Anatomy of organ of corti. From [33].

On top of the basilar membrane is the organ of corti, which contains sensitive receptor cells called inner and outer hair cells. On the apical side of the inner hair cell sits the stereocilia bundle (Fig. 3a), which is responsible for detecting fluid vibration in the cochlear duct[9].

The stereocilia tips of outer hair cells are embedded in the tectorial membrane and detect movement of the basilar membrane relative to the tectorial membrane. The stereocilia rows arrange in order of increasing height and are connected to each other by a filamentous structure called the tip link[10] (Fig. 3b-d). Mechanical force from sound causes the stereocilia to deflect, thereby stretching the tip links and opening nearby transduction channels[11]. When stereocilia bends in the direction of the tallest stereocilium, tip links stretch; mechanotransduction ion channels then open and allow potassium ions to enter the cell. The influx of potassium ions causes the cell to depolarize and generate action potentials in afferent neurons. When stereocilia bundle bends in the direction of the shortest stereocilium, tip links slack; mechanotransduction ion channels then close and stop the potassium current. The cell then hyperpolarizes and neurotransmitter release decreases or stops. The tip link consists of two proteins: Protocadherin-15 (PCDH15) and Cadherin-23

(CDH23), which are essential for hearing and belong to the cadherin superfamily of proteins.

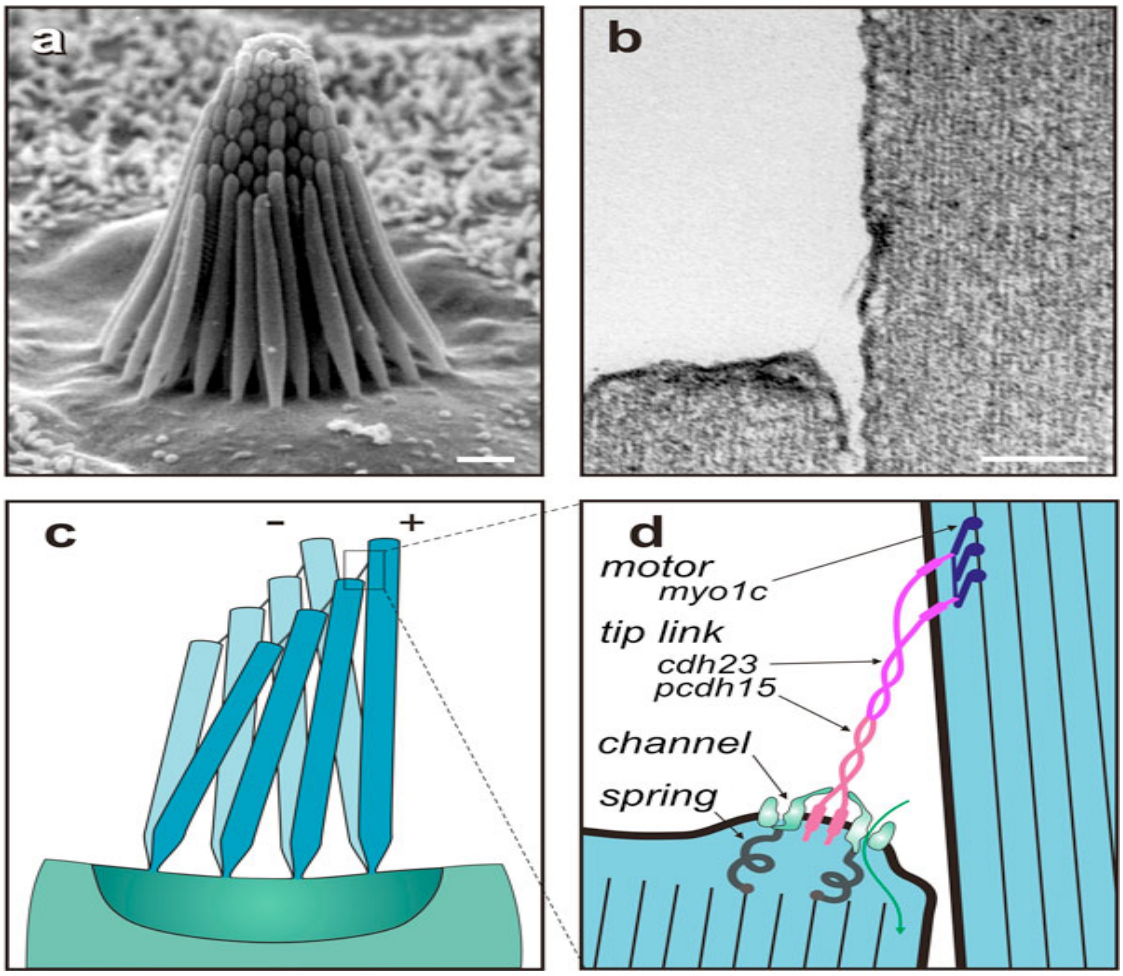

Figure 3: Mechanotransduction in vertebrate hair cells
(a) Hair cell stereocilia align in increasing height toward the tallest stereocilia, which defines the excitatory axis. (b) Tip link structure consists of CDH23 and PCDH15 and connects the top of one stereocilia to the side of its tallest neighbor. (c) Stereocilia deflect during mechanotransduction. (d) A close up look of the tip-link region with ion channels located at the lower end of each tip link. Adapted from [30].

1.2 The cadherin superfamily of proteins and the role of calcium

The cadherin superfamily includes classical cadherins, as well as clustered and non-clustered protocadherins, all with extracellular cadherin (EC) repeats[12,13]. Cadherins can be seen as a significant component of various living multicellular organisms, which plays an important role in cell signaling and mechanical processes[13]. The structure of cadherin has been recognized as EC "repeats" that position in series with calcium ions in between the EC repeats that modulate their elasticity and mediate its cell-cell adhesion ability[14]. The function of calcium ions, which support the structural integrity of cadherin's linker regions, has been studied using biochemical and computational tools[15–17].

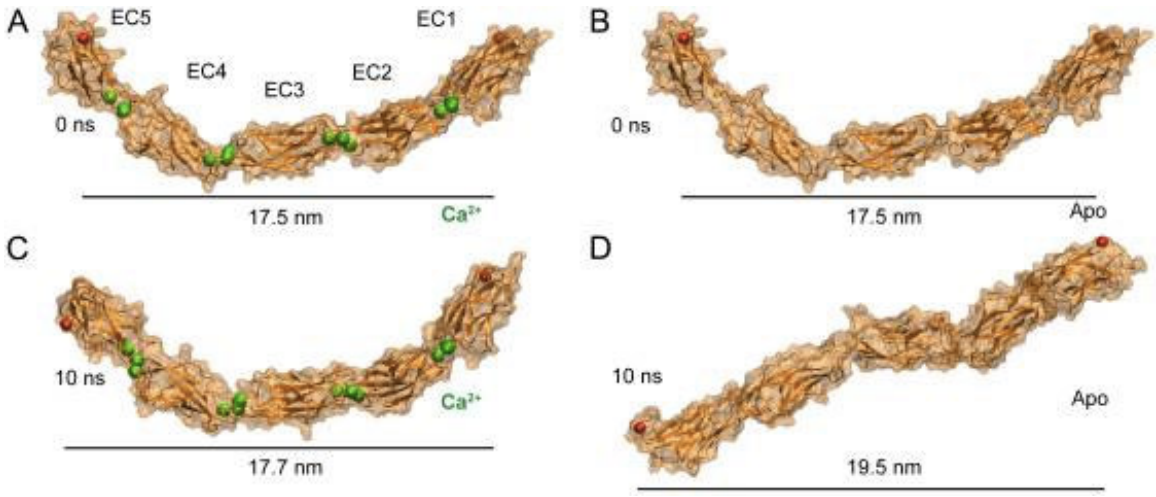

Figure 4: Calcium ions impact C-cadherin conformation. Simulations of the complete C-cadherin extracellular domain with and without Ca^{2+} ions, respectively (A and B). The protein is shown in cartoon representation and its surface is drawn in transparent orange. Green and red spheres are crystallographic Ca^{2+} and terminal C_α atoms. Screenshots of the complete extracellular domain of C-cadherin after 10 ns of equilibration in the presence of Ca^{2+} ions (C), in the absence of Ca^{2+} ions (D), respectively. While C-cadherin remains curved when simulated in the presence of Ca^{2+}, its shape is lost after 10 ns of dynamics in the absence of Ca^{2+}. Adapted from [16].

The result shows that the extracellular domain is capable of maintaining its crystal conformation with calcium ions by forming an elongated and curved structure,

while its structure is flexible without the presence of calcium ions[16]. Thus, calcium ions are essential for cadherin to establish and maintain its proper conformation.

1.3 Tip link interactions and structure of CDH23 and PCDH15 tips

Hair cells are the mechanosensors responsible for transducing mechanical forces originated from sound waves and head movements[1]. Hair cells then convert the mechanical forces into electrochemical signals, which can be sent to the brain through the auditory nerve[1]. The mechanoelectrical transduction channel locates near the tips of stereocilia, where the extracellular tip-link filaments are located[18,19]. This fine filament structure is composed of two proteins, CDH23 and PCDH15, whose mutations are known to cause deafness[20,21,7]. Crystallography and molecular dynamics simulations studies have been conducted to determine how CDH23 binds to PCDH15. A unique "handshake" model has been found to be the cadherin interaction mechanism, in which an antiparallel heterodimer between the two most amino-terminal cadherin repeats (EC repeats 1 and 2) of each protein is formed[22].

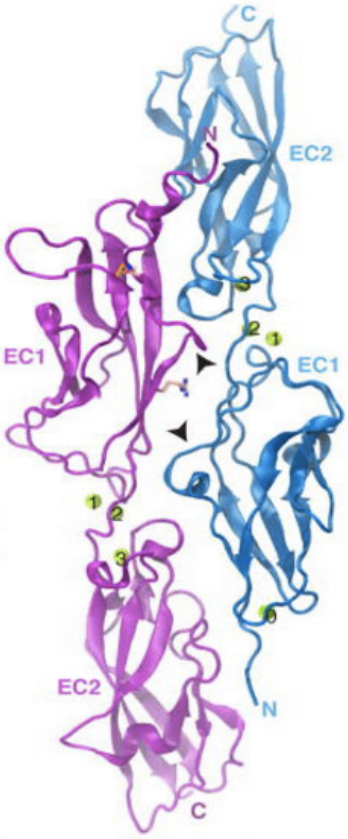

Figure 5: Ribbon diagram of PCDH15 EC1+2 (purple) interacting with CDH23 EC1+2 (blue) with Ca^{2+} ions as green spheres. Adapted from [22].

The complex is calcium-dependent, as these ions provide rigidity and facilitate the handshake interaction. Multiple missense mutations at calcium binding sites and at the handshake interface are known to cause deafness[7,22].

1.4 PCDH15 EC7-8

PCDH15 is one of the non-classical members of the cadherin superfamily that have multiple EC repeats. There have been vast studies focusing on classical cadherins, but we only have limited knowledge about the non-classical cadherins, such as PCDH15. To our knowledge, the structure of PCDH15 EC4-11 has never been discovered. Thus, by studying the EC7-8, it could allow us to have a further insight of this cadherin complex.

Figure 6: Cartoon display of PCDH15 EC repeats with EC7-8 marked in red.

Based on the structure of PCDH15 EC1-2, we predict that PCDH15 EC7-8 is about 200 amino acids in length, which weighs about 24 kDa. A point mutation in EC7 is known to cause non-syndromic deafness[23]. In addition, we also find an interesting variation in EC7 at one of its calcium-binding motifs (DYE). Resolving the structure of PCDH15 EC7-8 will allow us to understand the role of the deafness mutation in EC7, the structural implications of the sequence variation in EC7's calcium-binding motifs, and also possible parallel dimers of PCDH15.

Chapter 2: Producing the protein

Hearing is extremely important for vertebrate life, and here we focus on the structures of tip link proteins that are essential for inner-ear mechanotransduction. Studying the structure of protocadherin-15 (PCDH15) fragments that form part of the tip link could allow us to have a better understanding of its role in hearing mechanotransduction. Our group has studied the tip-link interaction involving small PCDH15 and CDH23 tips, but the whole structure of PCDH15 has not been solved yet. Thus, our group has designed various constructs to express and purify fragments of PCDH15. I worked with one of them encoding for *Mus musculus* PCDH15 EC7-8, and used it for expression, purification and crystallization as described in this chapter.

2.1 Cloning, propagation, and sequencing of mmPCDH15EC7-8

The *Mus musculus* PCDH15 cDNA was used as the source for cloning PCDH15 EC7-8 into the pET21a vector (cloning performed by Dr. Sotomayor and co-workers). The fragment construct was designed by using the published structure of PCDH15 EC1-2 as a reference (Protein Data Bank code 4APX). Dr. Sotomayor designed primers that allowed amplification of the desired fragment and included the sequence of NdeI and XhoI restriction enzyme sites. After amplification using PCR, the restriction enzymes NdeI and XhoI were used to digest the amplified sequence (PCR product), which was then ligated to a digested plasmid vector pET21a(+). The pET21 vector carries an ampicillin resistance gene, an isopropyl β-D thiogalactopyranoside (IPTG)

inducible T7 promoter, and a C-terminal six-histidine tag to allow for Ni-affinity purification of the expressed gene fragment. I used DH5α *E. coli* cells and standard "miniprep" protocols to propagate and obtain more mmPCDH15EC7-8 DNA plasmid. The length of the insert was verified by NdeI and XhoI enzyme digestions and agarose gel analysis. In addition, the plasmid was sequence verified with the T7 promoter and T7-terminator primers.

2.2 Protein expression of PCDH15 EC7-8

BL21-Gold (DE3) *E. coli* cells were used to express the PCDH15 EC7-8 construct. These cells contain the T7 polymerase gene and have been modified for high efficiency protein production. All BL21 cells were grown in Lysogeny Broth (LB) medium.

To test for protein expression, single colonies of transformed BL21 cells were inoculated and grown overnight. Then, a small amount of 25 mL expression culture with 100 µg/mL of ampicillin was inoculated with 200 µl of the overnight culture and incubated at 37 °C until the culture reached an OD_{600} of 0.6, at which point IPTG was added for a final concentration of 200 µM. The cells were grown at 37 °C with shaking overnight, and were then pelleted by centrifugation. A small sample of pellets was resuspended in SDS loading buffer and boiled for denaturation. The sample was then loaded onto a SDS-PAGE gel and stained with Coomassie to determine the expression of the protein fragment of interest. Protein expression for mmPCDH15 EC7-8 was successful (Fig. 7). The PCDh15 EC7-8 protein was then expressed at a larger scale for further biochemical assessments and crystallization

assays. A 2 L large culture was inoculated with 25 mL of overnight BL21 cell culture. The liquid medium was preheated to 37 °C for optimal growth prior to the addition of the cell culture. The large culture was then grown until the OD_{600} reached 0.6, induced with IPTG (200 μM final concentration), and incubated overnight at 37 °C. On the following day, the cells were collected, pelleted, and stored at -20 °C.

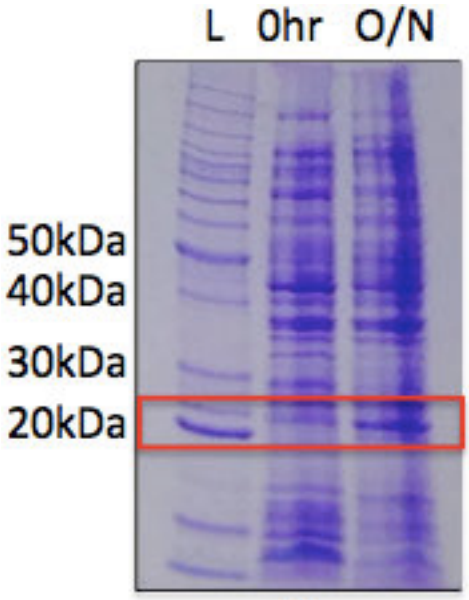

Figure 7: Protein expression result of PCDH15 EC7-8 at 37 °C at 0hr vs. overnight. Molecular weight of PCDH15 EC7-8 is ~24 kDa, marked in red.

2.3 Purification and one-step refolding of PCDH15 EC7-8

Protocadherins have a tendency to form inclusion bodies. Thus, PCDH15 fragments were purified under denaturing conditions. Sonication was first used to lyse the pelleted cells with a denaturing binding buffer (20 mM Tris-HCl pH 7.5, 10 mM $CaCl_2$, 6 M guanidinium hydrochloride, and 20 mM imidazole pH 7.5). Roughly 35 mL of binding buffer was added to 6 g of cell pellet. The lysate was then centrifuged at 20,000 rpm for 30 minutes at 4 °C to wash off any cellular debris. After centrifugation, the protein-rich supernatant was incubated with Ni-sepharose high performance beads for one hour at 4 °C. After incubation, the mixture was centrifuged again at 3,000 rpm for 5 minutes at 4 °C and the supernatant was decanted. The Ni beads were washed again and the mixture was then placed in the

denaturing elution buffer with high imidazole concentration (20 mM Tris-HCl pH 7.5, 10 mM $CaCl_2$, 6 M guanidinium hydrochloride, and 500 mM imidazole pH 7.0) to elute the protein (Fig. 8).

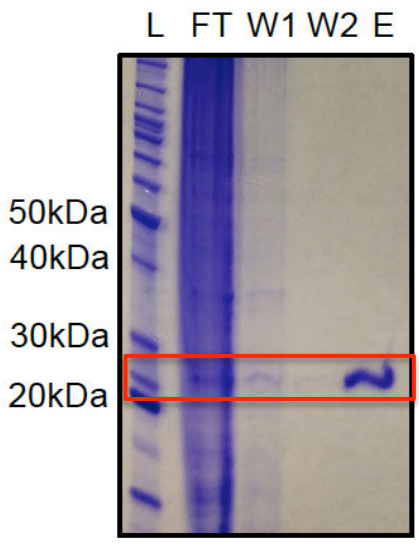

Figure 8: Protein purification result analyzed by SDS-PAGE. First lane: Protein ladder. Second lane: flow through. Third lane: first wash with binding buffer. Fourth lane: second wash with binding buffer. Fifth lane: Protein elution. Molecular weight of PCDH15 EC7-8: 24 kDa.

To refold PCDH15 EC7-8, the protein elution was diluted with denaturing elution buffer to a concentration of < 0.5 mg/mL. The diluted protein was dialyzed at 4°C overnight using buffer D (20 mM Tris-HCl pH 8.0, 5 mM $CaCl_2$, 150 mM KCl, 5 mM $CaCl_2$, 10% Glycerol), which dilutes guanidinium hydrochloride from the protein solution to promote refolding of the protein fragment. We found that glycerol was able to assist PCDH15 EC7-8's refolding by preventing protein precipitation. After overnight dialysis, the protein solution was collected and centrifuged at 20,000 rpm for 30 minutes at 4 °C to remove precipitations. After centrifugation, the protein solution was concentrated with a 10,000 MWCO filter (polyethersulfone membrane) to concentrations ranging between 3 to 9 mg/mL for future size-exclusion chromatography (SEC) and subsequent protein crystallization.

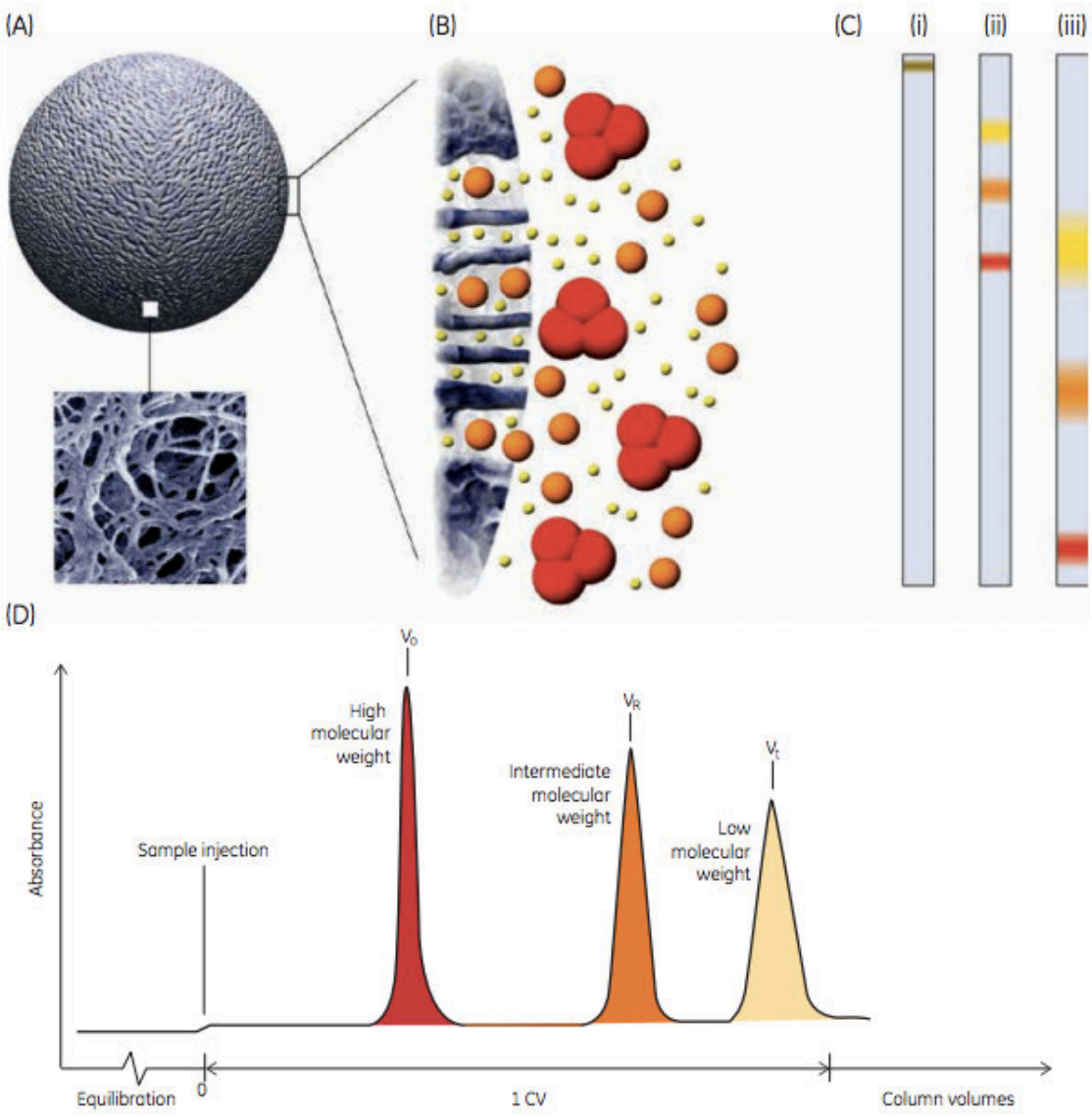

Figure 9: Process of size-exclusion chromatography (SEC). (A) Schematic picture of a bead with an electron microscopic enlargement. (B) Schematic drawing of sample molecules diffusing into bead pores. (C) Graphical description of separation: (i) sample is applied on the column; (ii) the smallest molecule (yellow) is more delayed than the largest molecule (red); (iii) the largest molecule is eluted first from the column. (D) Schematic chromatogram. Adapted from [34].

2.4 Purification of PCDH15 EC7-8

The protein was further purified by SEC (Figs. 9 & 10) with a S200 Superdex 16/60 GL (GE Healthcare) column and buffer containing 20 mM Tris HCl pH 8.0, 150 mM KCl and 5 mM $CaCl_2$. This method separates protein based on size, as the porous resin of the column traps and delays proteins with low hydrofluidic volume while larger proteins bypass the pores and are eluted out faster. The concentrated protein solution was filtered before loading onto the column by using a 0.45 µm PES membrane. After SEC, I used Coomassie-stained SDS-PAGE to determine the purity and integrity of the eluted fractions (Fig. 10B).

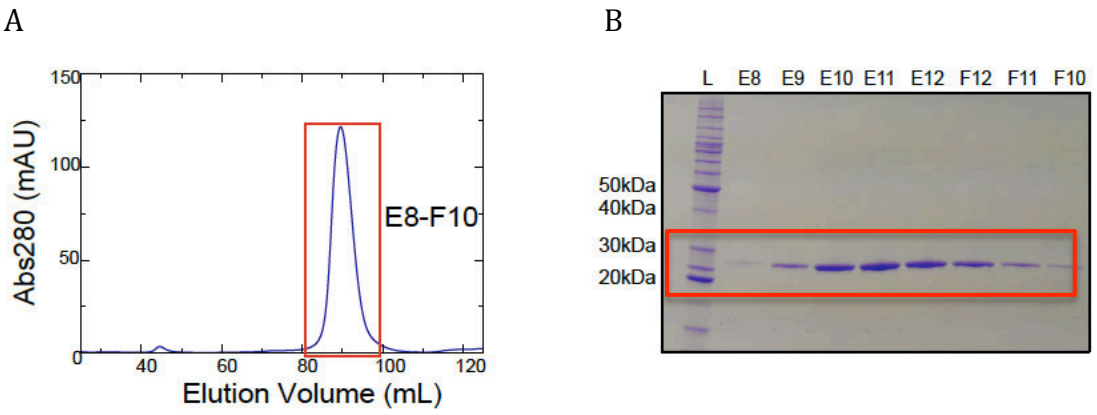

Figure 10: Size-exclusion chromatography result of refolded PCDH15 EC7-8 (A) and SDS-PAGE gel analysis of peaks (B).

Chapter 3: Crystallization and Data Collection

Protein crystallization can be achieved under suitable conditions in which protein molecules form repeating patterns by non-covalent interactions within the protein crystal[24]. There are numerous variables that can affect the sensitivity of protein crystallization ability, such as temperature, ionic strength, protein concentration and pH[25]. Additionally, the growth of protein crystals also requires different time periods and it is nearly impossible for us to predict exact crystallization conditions a priori.

In this chapter, I will explain how I crystallized PCDH15 EC7-8 and how I designed a refinement screen to search for good diffracting crystals. After successful crystallization, we shot the crystals with X-rays, obtained a complete data set, and used molecular replacement to determine the PCDH15 EC7-8 structure. Our final model at 2.0 Å resolution shows for the first time the architecture of these EC repeats, including canonical calcium-binding sites at the linker between EC7 and EC8 and the location of sites that are mutated in hereditary deafness.

3.1 Crystallization of PCDH15 EC7-8

To carry out X-ray crystallography on PCDH15 EC7-8, I expressed and purified this protein fragment as described in chapter 2. The protein fragments were then concentrated to 4 mg/mL and 7 mg/mL, and dispensed on a 96-well sitting drop tray, which contained a larger well for reservoir solution and a smaller well for purified protein mixed with reservoir solution (Fig. 11). The protein fragment EC7-8

was crystallized by sitting drop vapor diffusion method, which required both the reservoir buffer and purified protein to be within a closed system.

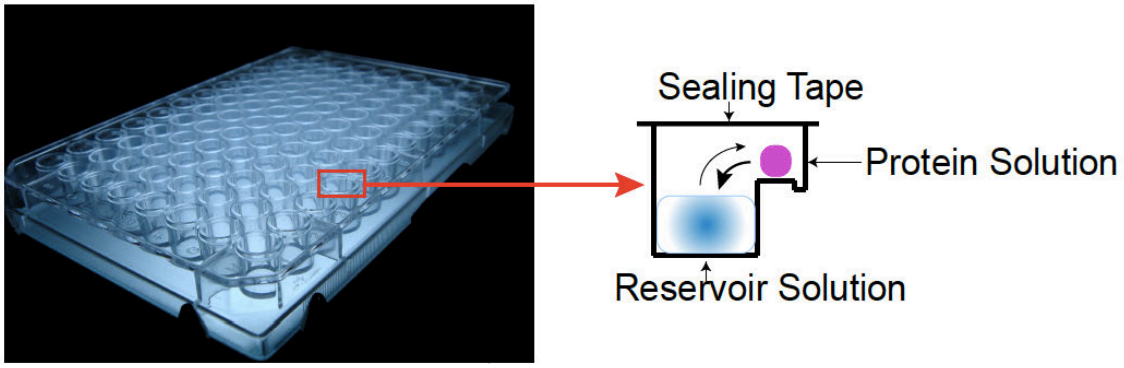

Figure 11: Protein crystallization by sitting drop vapor diffusion method. Adapted from [35].

The sitting drop utilized the principle of vapor diffusion between the reservoir buffer and purified protein solution, where water in the purified protein solution vapors into the reservoir buffer in order to balance concentration and reach an optimal condition for protein crystallization[26,27]. At first, I used three different buffer suites to determine the best conditions for my protein construct's crystallization: QiAGEN classics, PEG (polyethylene glycol), and cation suites. I added 75 µL of reservoir buffer into the bigger well, 0.6 µL of purified protein solution into the smaller well, and transferred 0.6 µL of reservoir buffer into the smaller well. The trays were then sealed with plastic tape and stored at 4 ^{o}C. The protein crystallized approximately after one month of setting up the trays. I closely monitored protein growth under the optical microscope during this month. The protein crystallized in several of the PEG suite conditions at the concentration of 4 mg/mL (Fig. 12).

Crystals of PCDH15 EC7-8	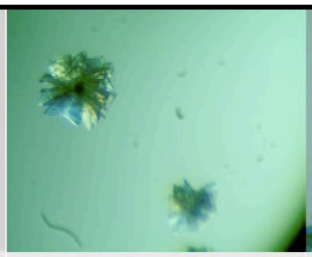	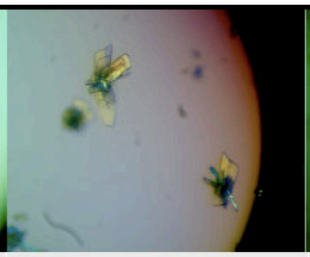	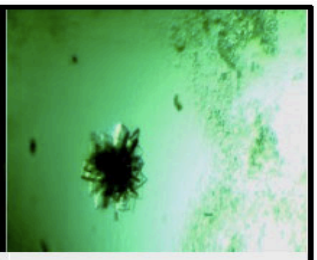
Pre-Screen Suite	PEG	PEG	PEG
Condition	0.1 M MES pH6.5 15% PEG 20000	0.2 M NH_4Cl 20% PEG 3350	0.2 M $(NH_4)_2SO_4$ 20% PEG 3350

Figure 12: Protein crystals in pre-screen PEG suite under different conditions.

Dr. Marcos Sotomayor "fished" the protein crystal with a 0.05 mm loop and shot the protein crystal with X-rays using the home source at the first floor of the Riffe building (RigakU MicroMax 003). The diffraction pattern indicated that we had a protein crystal, so the protein crystal was saved in liquid nitrogen for future analysis at APS (Advanced Photon Source) in the Argonne National Laboratory.

3.2 Refinement of PCDH15 EC7-8 crystallization conditions

Based on the protein crystallization condition mentioned above, I designed my refinement screen to provide an optimal set of conditions for crystal growth (Fig. 13). The crystals I observed that were best for X-ray diffraction were grown in ammonium chloride with PEG 3350, ammonium sulfate with PEG 3350, MES with PEG 20000, and ammonium sulfate with glycerol and PEG 3350. I used different concentrations of PEG 3350, PEG 20000, ammonium chloride and ammonium sulfate, as well as MES at various pH.

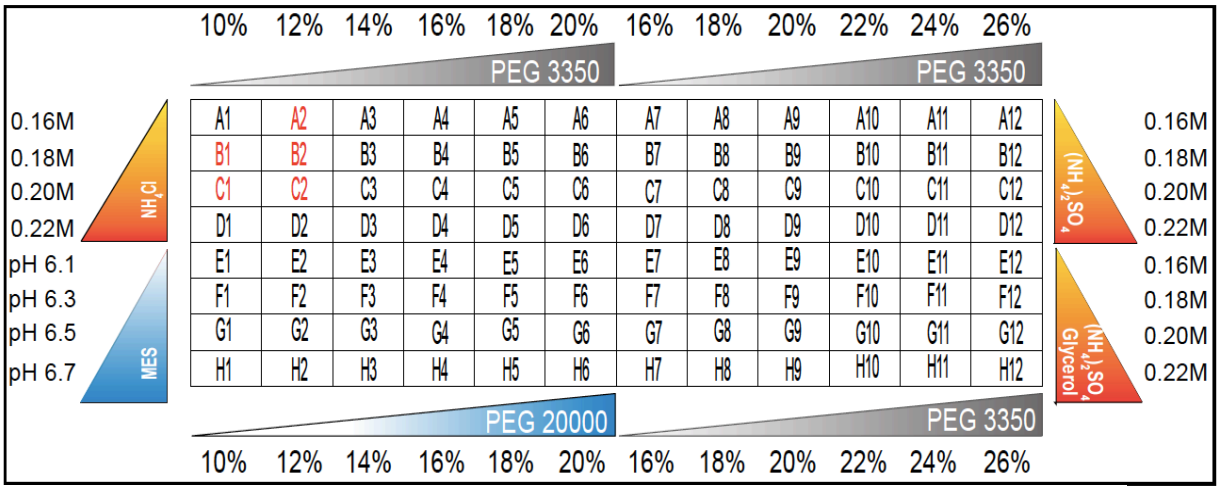

Figure 13: Refinement screen for PCDH15 EC7-8 crystallization.

After monitoring the growth of protein crystals in this refinement, I suggested that the protein grew best in ammonium chloride and PEG 3350, where the best conditions are shown in red in Figure 13.

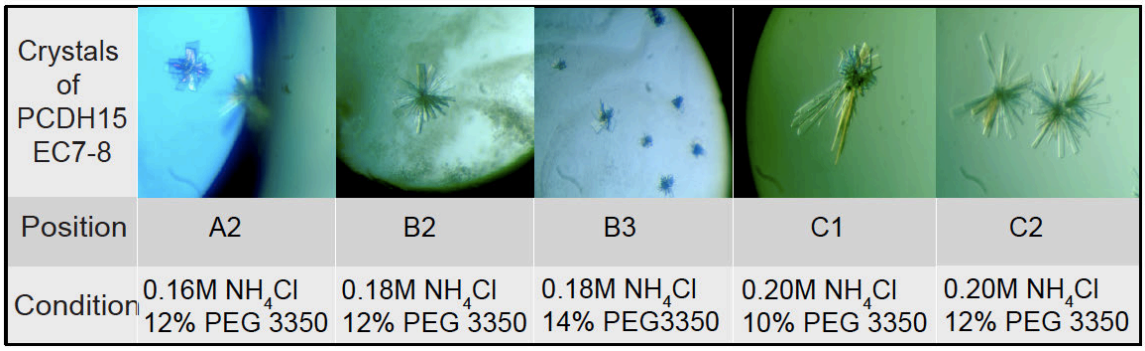

Figure 14: Protein crystals of PCDH15 under refinement conditions.

These crystals were fished by Dr. Marcos Sotomayor and sent to APS (Advanced Photon Source) at Argonne National Laboratory.

3.3 Diffraction data collection of PCDH15 EC7-8

The diffraction data for EC7-8 crystals were collected on the beamline of the Advanced Photon Source (APS) at Argonne National Laboratory. Dr. Marcos Sotomayor assisted me to index, integrate and scale the diffraction data with HKL 2000.

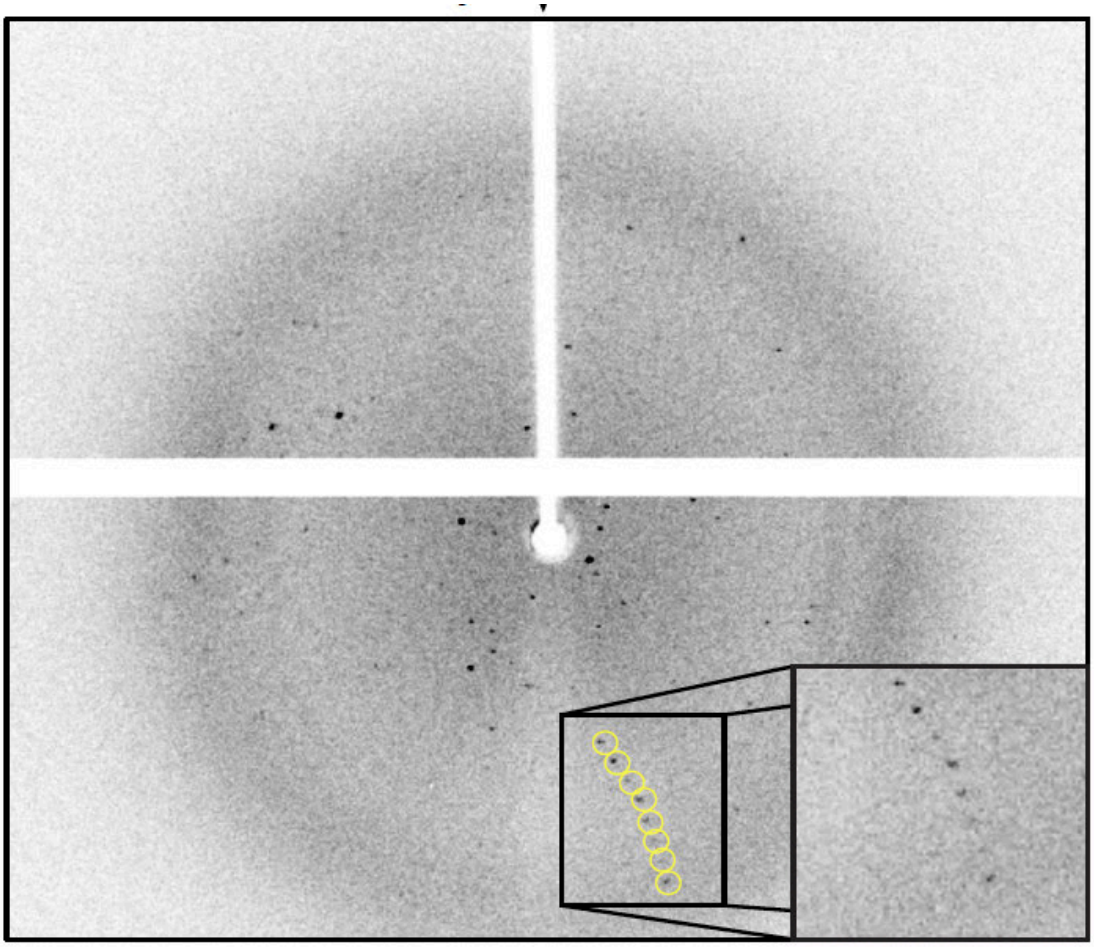

Figure 15: Diffraction of PCDH15 EC7-8. PCDH15 EC7-8 crystals (Figure 13-B2) grew in a refinement condition containing 10% ammonium chloride and 0.2 M PEG 3350 and diffracted to high resolution and exhibited no signs of twinning, making structure determination feasible. The diffraction image is the dataset that was used to determine the structure of the EC7-8 fragment.

The best diffraction data we got was under the condition of 0.2 M ammonium chloride and 10% PEG 3500 with final resolution of 2.0 Å. The space group we observed was C_12_1. Preliminary statistics for data collection and refinement are shown in Table1 below.

Data collection	MmPCDH15 EC7-8
Space group	C_12_1
Unit cell parameters	
a, b, c (Å)	135.796, 22.99, 70.741
α, β, γ (°)	90, 97.268, 90
Molecules per asymmetric unit	1
Beam source	APS-24-ID-C
Wavelength (Å)	0.9792
Resolution limit (Å)	2.000
Unique reflections	14026
Completeness (%)	96.5 (82.1)
Redundancy	3.1 (2.4)
I / $\sigma(I)$	5.4
R_{merge}	0.045
R_{meas}	0.054
R_{pim}	0.030
$CC_{1/2}$	(0.974)
CC^*	(0.993)
Refinement	
Resolution range (Å)	50.00-2.00 (2.03 – 2.00)
R_{work} (%)	0.1796
R_{free} (%)	0.2414
Residues (atoms)	212 (1575)
Water molecules	110
Rms deviations	
Bond lengths (Å)	0.0173
Bond angles (°)	1.8342
B-factor average	41.78
Protein	41.80
Ligand/ion	34.94
Water	41.52
Ramachandran Plot Region (PROCHECK)	
Most favored (%)	87.9
Additionally allowed (%)	10.3
Generously allowed (%)	0.0
Disallowed (%)	0.0

Table 1: Preliminary statistics for data collection of PCDH15 EC7-8. The numbers present the information of complete data set. The numbers in parentheses indicates the high-resolution shell.

3.4 Data processing and structure determination for PCDH15 EC7-8

The macromolecular model of PCDH15 EC7-8 was built using Coot (Crystallographic Object-Oriented Toolkit) and an initial model of PCDH15 EC8-10 by Dr. Raul Araya-Secchi. We made use of the PCDH15 EC8 model to do molecular replacement, obtain initial phases, and build the whole EC7-8 structure.

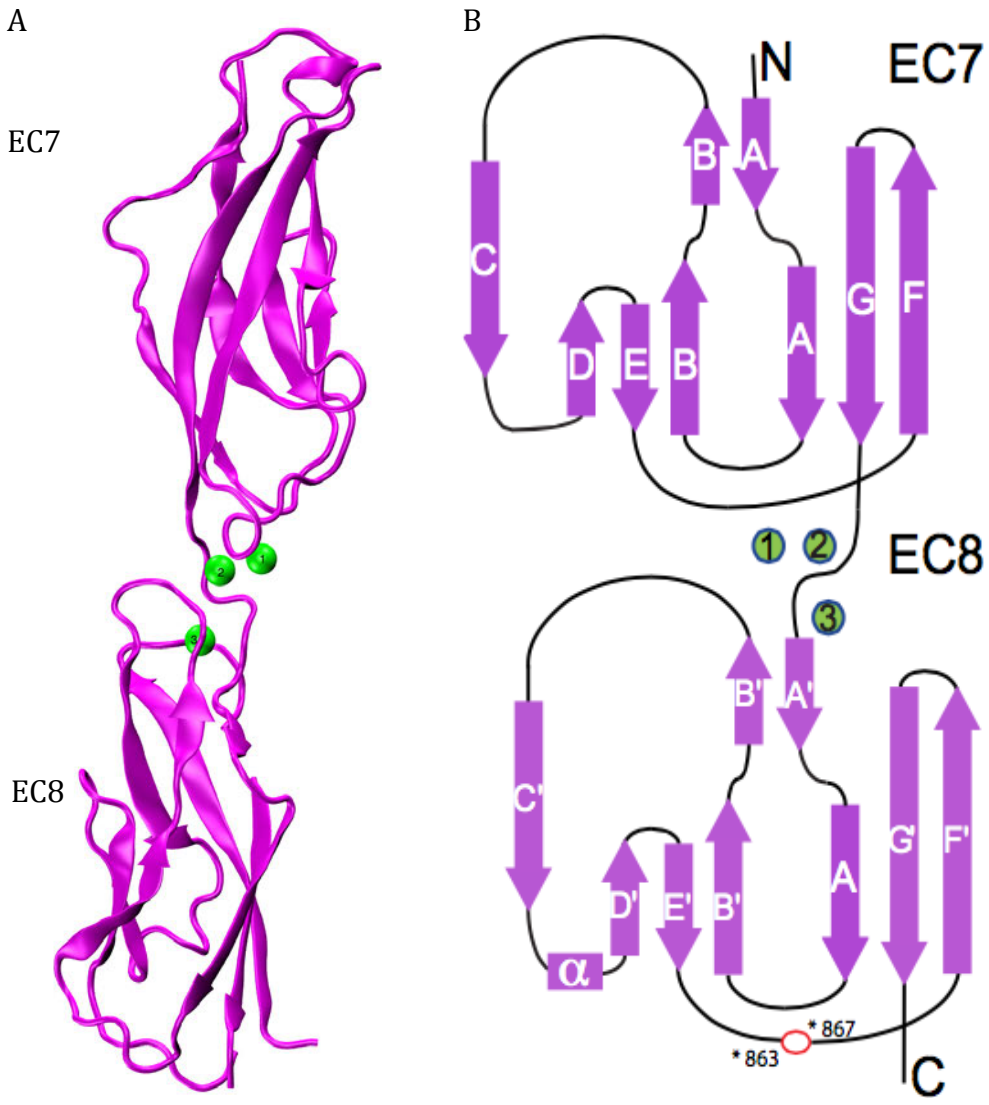

Figure 16: (A) Structure of PCDH15 EC7-8 visualized by VMD. (B) Topology diagram of PCDH15 EC7-8. The missing residues are indicated in red.

As we built the model, we used the software Refmac to do reciprocal space refinement. The current R-factor is 0.18 and the R_{free} factor is 0.24, which indicate the agreement between our crystallographic model and the experimental data. The relatively small R factor of 0.18 implies a minor dissimilarity between experimental observations and theoretical calculated values.

Chapter 4: Structure Analysis

The studies in this thesis represent the initial stages of the structural characterization of PCDH15 EC7-8 with its calcium-binding linker region. After optimizing expression, refolding, and purification protocol for PCDH15 EC7-8, I successfully crystalized and determined its structure. The structure reveals that the linker region between EC7 and EC8 in PCDH15 binds three Ca^{2+} ions, which is the canonical binding mode previously observed in the majority of cadherin structures. In this chapter, I will analyze this canonical calcium dependent structure and its calcium binding sites. Next, I will talk about the site within PCDH15 that is known to cause deafness when mutated. Then I will discuss interesting interfaces that are formed by crystal contacts of PCDH15 EC7-8. Finally, I will discuss the implications of the results observed in this study, and propose further experiments that are aimed not only at reproducing these results, but also at gaining a better understanding of non-classical cadherins.

4.1 Calcium binding sites in cadherins

There are five conserved calcium-binding motifs between the EC repeats in cadherins in general. The complete sequence alignment of the 11 EC repeats of PCDH15 is shown below (Fig. 17) and shows the presence or absence of these motifs in this protein[28].

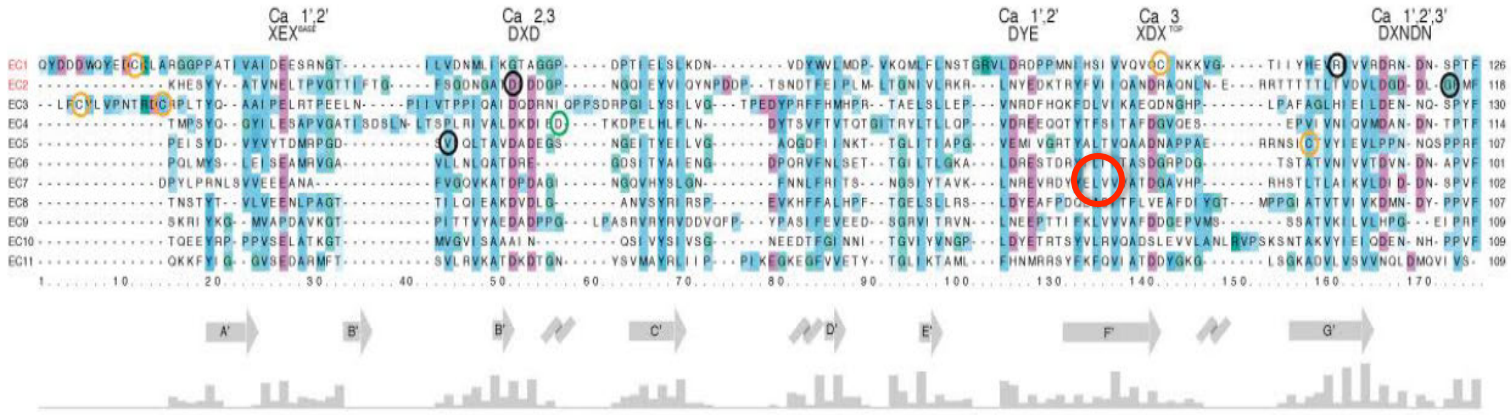

Reference	Mutation Gene #	Structure #	Cadherin Repeat #	Calcium Binding Motif
Ahmed et al. 2003	D139G	D113G	EC1	
Ahmed et al. 2008	D183G	D157G	EC2	**D**XD
Ahmed et al. 2003	G262D	G241D	EC2/EC3	DXNDN**X**
Doucette et al. 2009	V533D	V507D	EC5	
Grossman et al. 2010	D440A	D414A	EC4	

Figure 17: Alignment of PCDH15 EC repeats of interest for this thesis. Mutations linked to deafness are circled in red. Amino acid motifs forming calcium-binding sites are shown above alignment (XEX^{BASE}, DXD, DRE, XDX^{TOP}, DXNDN). Adapted from [28].

There are five calcium-binding motifs within PCDH15 extracellular repeats. The first binding motif is the XEX^{BASE}, the second one is the DXD, the third one is the DRE, the fourth one is the XDX^{TOP} and the last one is DXNDN. The letter "X" indicates any non-conserved amino acids, while the preserved amino acid, such as the E in the first calcium-binding motif, indicates its interaction with the calcium ions within the repeats. Those five calcium-binding motifs work together to maintain the structure of PCDH15 and to determine its elasticity.

4.2 Analysis of PCDH15 EC7-8 structure

Based on our molecular replacement solution and refinement, we obtained the molecular structure of PCDH15 EC7-8 (Fig. 16), which is similar to the structure of other cadherin molecules. The EC7-8 fragment contains 209 amino acids in total, which correspond to residues 692 to 897. We were able to place the majority of the amino acids, water molecules and three calcium ions in the electron density. Chain A contains major amino acids of our protein fragment, chain B contains calcium ions and chain C contains water molecules. There were still a few missing residues starting from residue 863 to 867 that we were unable to place because of the lack of electron density. According to the molecular structure, there were three calcium ions between EC7 and EC8. The first calcium is coordinated by Glu 708, Asn 757 and Glu 759, the second calcium is coordinated by Glu 759, Asp790, Asn 794 and Glu 826 and the third one is coordinated by Asp 792, Asp 824 and Asp 826. The structure of EC7-8 is conserved and similar to that of PCDH15 EC1-2[22].

4.3 Location of deafness site

PCDH15, essential for the auditory system, is known as a non-classical cadherin with a large extracellular domain that is involved in hereditary deafness. The most frequent cause of blind-deafness in humans, Usher syndrome, is related to genetic mutations that modify PCDH15 among other proteins. An unusual point mutation locates in PCDH15 EC7 at V767-, where the in-frame deletion of this valine is known to cause inherited non-syndromic deafness DFNB23[23].

Mutated	REVRDYYEL-VVATDGAVHPRH
H.sapiens	REVRDYYELVVVATDGAVHPRH
P.troglodytes	REVRDYYELVVVATDGAVHPRH
M.mulatta	REVRDYYELVVVATDGAVHPRH
C.lupus	REVRDYYELVVVATDGAVHPRH
B.taurus	REVRDYYELVVVATDGAVHPRH
M.musculus	REVRDYYELVVVATDGAVHPRH
R.norvegicus	REVRDYYELVVVATDGAVHPRH

Figure 18: Mutated sequence (V767-) in PCDH15, which is highly conserved in mammalian species. Adapted from [23].

The point mutation locates between the third Ca^{2+} binding motif (DYE) and the fourth Ca^{2+} binding motif (XDX^{TOP}) as shown below (Fig. 19), and does not directly affect calcium binding (the point mutation is circled in red).

Figure 19: Partial sequence alignment of PCDH15 EC repeats with point mutation V767- circled in red. Adapted from [31].

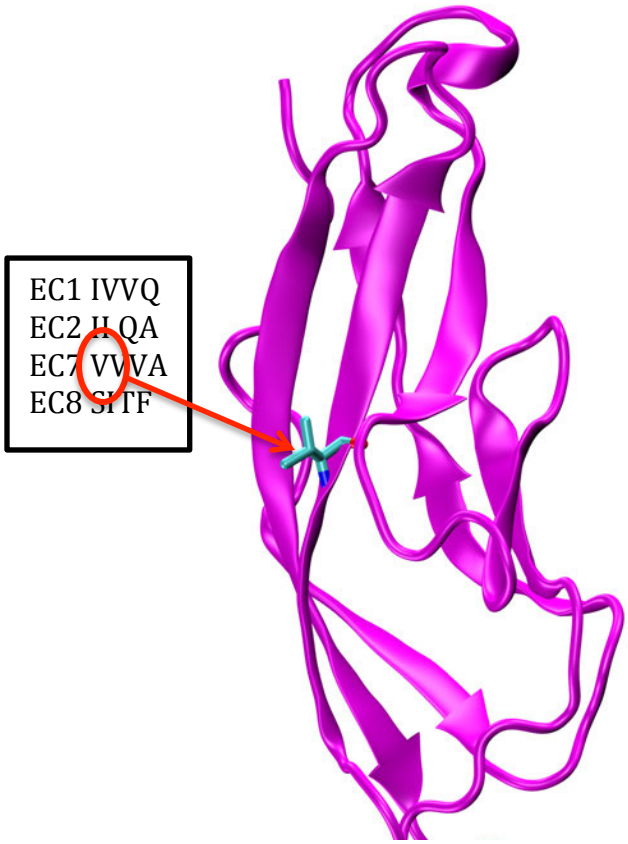

Figure 20: Point mutation in PCDH15 EC7 visualized in VMD.

As we have solved the structure of PCDH15 EC7-8, we are able to locate the point mutation within our sequence to know how would the mutation affect the crystallized structure (Fig. 20). We are also able to know how the point mutation could interfere within the crystal contacts that may show physiologically relevant interfaces.

4.4 A potential PCDH15 parallel interface

After finalizing a preliminary model for PCDH15 EC7-8, we analyzed it with PDBePISA (Protein Interfaces, Surfaces and Assemblies) to determine possible intermolecular interfaces[29]. PISA suggests three feasible interfaces between EC7-8 units (Table 2 and Fig. 21).

PISA Interface List.

Session Map (id=613-L3-CHH)

Start | Interfaces | Interface Search

Monomers

Assemblies

Interfaces in CCP15EC7-8_1.1-coot-92.pdb crystal.

Space symmetry group: C 1 2 1

Interfaces | XML | View | Details | Download | Search

##		Structure 1				x	Structure 2					interface	ΔG	ΔG	N_{HB}	N_{SB}	N_{DS}	CSS
NN	« »	Range	N_{at}	N_{res}	Surface A^2		Range	Symmetry op-n	Sym.ID	N_{at}	N_{res}	Surface A^2	area, A^2	kcal/mol	P-value				
1	●	A	81	27	11131	◊	A	-x,y,-z	2_555	81	27	11131	750.6	3.8	0.955	10	4	0	0.000
2	○	A	78	30	11131	x	A	x,y-1,z	1_545	78	26	11131	741.9	-10.5	0.148	0	1	0	0.000
3	○	A	30	12	11131	x	A	-x-1/2,y-1/2,-z	4_445	34	12	11131	290.0	-2.3	0.509	1	0	0	0.000
4	○	[K]D:1	1	1	216	f	A	x,y,z	1_555	9	6	11131	114.2	-106.6	0.000	0	0	0	0.080
5	○	[CA]B:3	1	1	85	f	A	x,y,z	1_555	5	5	11131	42.8	-12.9	0.000	0	0	0	0.010
6	○	[CA]B:1	1	1	85	f	A	x,y,z	1_555	5	5	11131	40.1	-11.4	0.000	0	0	0	0.009
7	○	[CA]B:2	1	1	85	f	[CA]B:1	x,y,z	1_555	1	1	85	8.8	-2.7	0.000	0	0	0	0.002

Table 2: PISA interface list of PCDH15 EC7-8.

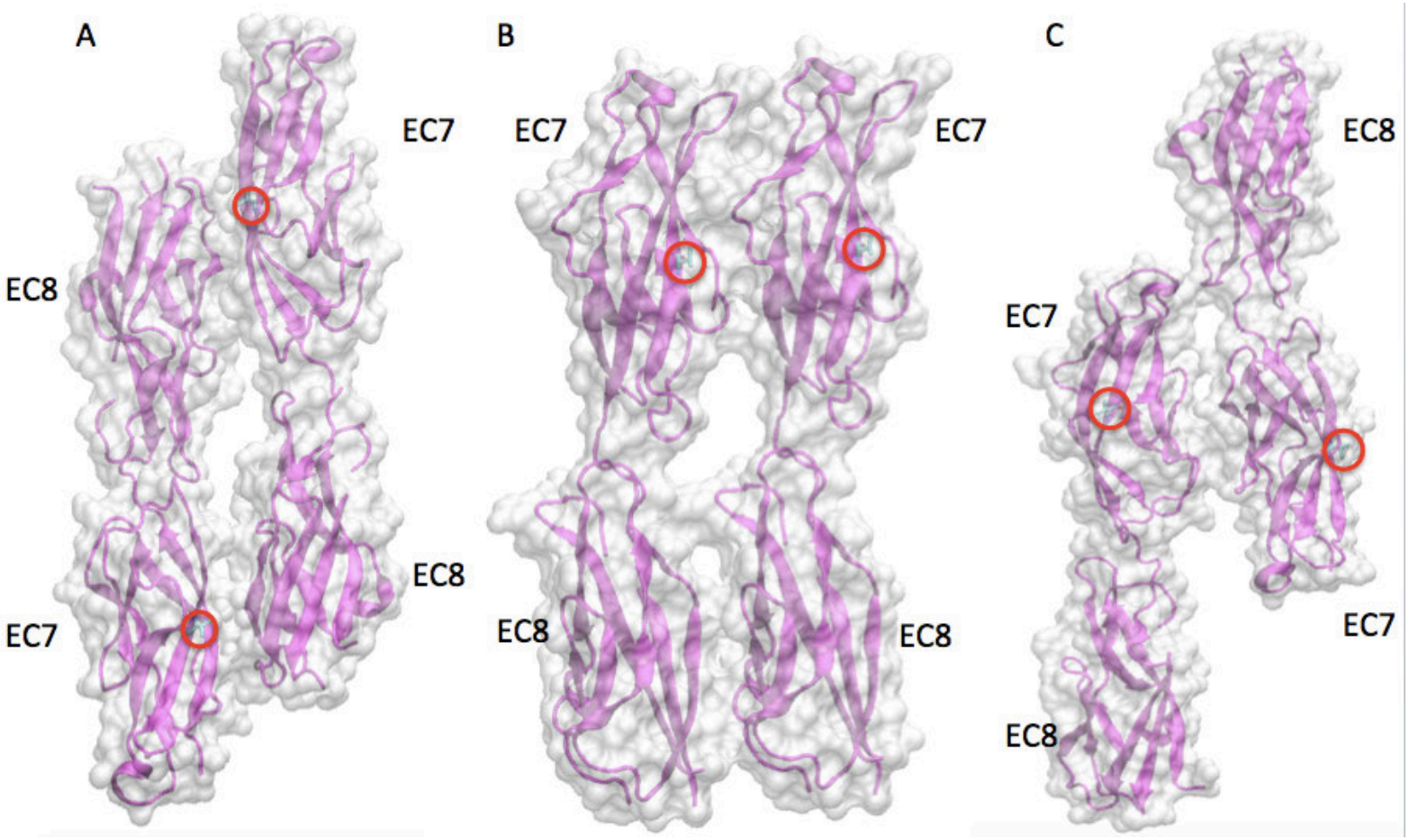

Figure 21: PISA analysis. (A) An antiparallel interface of PCDH15 EC7-8 indicated by PISA. (B) A parallel interface of PCDH15 EC7-8 indicated by PISA. (C) An antiparallel interface of PCDH15 EC7-8 indicated by PISA. The position of valine residue is circled in red.

The first result indicates an antiparallel interface area of 750.6 $Å^2$ with a ΔG P-value of 0.955. This large P-value indicates that the interface is likely to be a crystallography contact. The second result indicates a parallel interface with an interface area of 741.9 $Å^2$ and a ΔG P-value of 0.148. These small P-values indicate that the interface is more hydrophobic than usual crystallographic contacts and may exist in solution. The third result indicates an antiparallel interface with an interface area of 290 A^2 and a ΔG P-value of 0.509. This P-value indicates that the interface is nor surprising in terms of hydrophobicity. Because of its relatively small surface area compared to the previous two results, we discard it. Based on our preliminary result, we are still debating about the potential parallel and antiparallel interfaces of PCDH15 EC7-8. We believe that determining whether any of these interactions is valid would help us to have a better understanding of PCDH15 function and the structure of its entire extracellular domain.

4.5 The importance of studying non-classical cadherins

My structural analysis of the PCDH15 EC7-8 fragment reveals the canonical calcium ion stoichiometry and coordination mechanism of the EC7-8 linker region. The point mutation V767- provides us an opportunity to visualize the interaction of this deafness-related mutation and speculate about its mechanism[23]. Interestingly, by analyzing the crystal contacts, we may be able to detect possible interfaces. By finalizing the interface analysis, we could determine whether PCDH15 forms a parallel homodimer in which EC7 and EC8 form key contacts. To validate this

interface, crystal structures with more EC repeats are needed. An analysis of glycosylation sites is also needed.

References:

1. Müller, U. & Barr-Gillespie, P. G. New treatment options for hearing loss. *Nat. Rev. Drug Discov.* **14,** 346–365 (2015).
2. Nance, W. E. The genetics of deafness. *Mental Retardation and Developmental Disabilities Research Reviews* **9,** 109–119 (2003).
3. Cook, J. A. & Hawkins, D. B. Hearing loss and hearing aid treatment options. *Mayo Clin. Proc.* **81,** 234–7 (2006).
4. Robinson, J. Deafness. *Aust. Fam. Physician* **12,** 608–610, 612 (1983).
5. Géléoc, G. S. G. & Holt, J. R. Sound strategies for hearing restoration. *Science* **344,** 1241062 (2014).
6. Skarzynski, H., Lorens, A., Piotrowska, A. & Skarzynski, P. H. Hearing preservation in partial deafness treatment. *Med. Sci. Monit.* **16,** CR555–R562 (2010).
7. Ahmed, Z. M. *et al.* Mutations of the protocadherin gene PCDH15 cause Usher syndrome type 1F. *Am. J. Hum. Genet.* **69,** 25–34 (2001).
8. Ahmed, Z. M. *et al.* The tip-link antigen, a protein associated with the transduction complex of sensory hair cells, is protocadherin-15. *J. Neurosci.* **26,** 7022–7034 (2006).
9. Husbands, J. M., Steinberg, S. A., Kurian, R. & Saunders, J. C. Tip-link integrity on chick tall hair cell stereocilia following intense sound exposure. *Hear. Res.* **135,** 135–145 (1999).
10. Geisler, C. D. A model of stereociliary tip-link stretches. *Hear. Res.* **65,** 79–82 (1993).

11. Ashmore, J. Cochlear outer hair cell motility. *Physiol. Rev.* **88,** 173–210 (2008).

12. Hulpiau, P. & van Roy, F. Molecular evolution of the cadherin superfamily. *International Journal of Biochemistry and Cell Biology* **41,** 349–369 (2009).

13. Angst, B. D., Marcozzi, C. & Magee, A. I. The cadherin superfamily: diversity in form and function. *J. Cell Sci.* **114,** 629–641 (2001).

14. Harris, T. J. & Tepass, U. Adherens junctions: from molecules to morphogenesis. *Nat Rev Mol Cell Biol* **11,** 502–514 (2010).

15. Cailliez, F. & Lavery, R. Cadherin mechanics and complexation: the importance of calcium binding. *Biophys. J.* **89,** 3895–3903 (2005).

16. Sotomayor, M. & Schulten, K. The allosteric role of the Ca2+ switch in adhesion and elasticity of C-cadherin. *Biophys. J.* **94,** 4621–4633 (2008).

17. Pokutta, S., Herrenknecht, K., Kemler, R. & Engel, J. Conformational changes of the recombinant extracellular domain of E-cadherin upon calcium binding. *Eur. J. Biochem.* **223,** 1019–1026 (1994).

18. Spinelli, K. J. & Gillespie, P. G. Bottoms up: transduction channels at tip link bases. *Nat. Neurosci.* **12,** 529–530 (2009).

19. Fettiplace, R. & Kim, K. X. The physiology of mechanoelectrical transduction channels in hearing. *Physiol. Rev.* **94,** 951–86 (2014).

20. Sotomayor, M., Weihofen, W. A., Gaudet, R. & Corey, D. P. Molecular mechanics of tip-link cadherins. in *AIP Conference Proceedings* **1403,** 64–69 (2011).

21. Ahmed, Z. M. *et al.* Gene structure and mutant alleles of PCDH15: Nonsyndromic deafness DFNB23 and type 1 Usher syndrome. *Hum. Genet.* **124,** 215–223 (2008).

22. Sotomayor, M., Weihofen, W. a, Gaudet, R. & Corey, D. P. Structure of a force-conveying cadherin bond essential for inner-ear mechanotransduction. *Nature* **492,** 128–32 (2012).

23. Chen, D. ye *et al.* Mutation in PCDH15 may modify the phenotypic expression of the 7511T>C mutation in MT-TS1 in a Chinese Han family with maternally inherited nonsyndromic hearing loss. *Int. J. Pediatr. Otorhinolaryngol.* **79,** 1654–1657 (2015).

24. Rupp, B. & Wang, J. Predictive models for protein crystallization. *Methods* **34,** 390–407 (2004).

25. Helliwell, J. R. Protein crystal perfection and its application. in *Acta Crystallographica Section D: Biological Crystallography* **61,** 793–798 (2005).

26. Berman, H. M. The Protein Data Bank. *Nucleic Acids Res.* **28,** 235–242 (2000).

27. Drenth, J. & Mesters, J. *Principles of protein X-ray crystallography: Third edition*. *Principles of Protein X-Ray Crystallography: Third Edition* (2007). doi:10.1007/0-387-33746-6

28. Sotomayor, M., Weihofen, W. A., Gaudet, R. & Corey, D. P. Structural Determinants of Cadherin-23 Function in Hearing and Deafness. *Neuron* **66,** 85–100 (2010).

29. Bleuler, S., Laumanns, M., Thiele, L. & Zitzler, E. PISA—a platform and programming language independent interface for search algorithms. *Evol. multi-criterion Optim.* 494–508 (2003). doi:10.1007/3-540-36970-8_35

30. Corey, D. P. Cell biology of mechanotransduction in inner-ear hair cells. *F1000 Biol. Rep.* **1,** 58 (2009).

31. Geng, R. *et al.* Noddy, a mouse harboring a missense mutation in protocadherin-15, reveals the impact of disrupting a critical interaction site between tip-link cadherins in inner ear hair cells. *J. Neurosci.* **33,** 4395–404 (2013).

32. *U.S National Library of Medicine*. U.S. National Library of Medicine, n.d. Web. 09 Apr. 2016.

33. "OpenStax CNX." *OpenStax CNX*. N.p., n.d. Web. 09 Apr. 2016.

34. GE Healthcare. Size exclusion chromatography: Principles and Methods. GE Heal. Handbooks 139 (2012).

35. Growth, Solutions For Crystal. *Sitting Drop Vapor Diffusion Crystallization*(n.d.): n. pag. Web. 16 Mar. 2015.